OSL and RL of $LiMgPO_4$ crystals doped with rare earth elements

B. Marczewska#, A. Sas-Bieniarz, P. Bilski, W. Gieszczyk, M. Kłosowski, M. Sądel

Institute of Nuclear Physics Polish Academy of Sciences, PL-31-342 Kraków, Poland

ABSTRACT

$LiMgPO_4$ (LMP) doped with a combination of Tb, B, Eu, Er, Gd or Tm activators in form of the crystals grown by micro-pulling down process (MPD) was examined as optically stimulated luminescence detectors using continues wave and time-resolved modes (CW and TR-OSL) as well as radioluminescence (RL) under X-ray tube irradiation. The RL-OSL measurements were performed using a HELIOS-3 OSL reader with a 460nm diode light stimulation and 240-400 nm emission wavelength range for signal recording and compared with CW-OSL measured by Risoe reader. In TR-OSL mode the most sensitive samples were the crystals doped with Tb, B and doped with Tb, B, Er, in CW-mode the highest signal was recorded for crystal doped with Tb, B, Gd. The linear dose response was observed in the range from 0.5 to 10 Gy. RL signals measured for the dose rates of 62mGy/min of X-rays was very high for all investigated crystals, especially for the crystal doped with Tm and Tb, B. The highest RL signal was observed for the crystal doped with 1.2mol% of Tm.

Keywords: $LiMgPO_4$ (LMP), optically stimulated luminescence (OSL), time-resolved OSL (TR-OSL), radioluminescence (RL)

Corresponding author: Barbara Marczewska (e-mail: Barbara.Marczewska@ifj.edu.pl)

HIGHLIGHTS:

1. CW-OSL and TR-OSL investigation of $LiMgPO_4$ doped with Tb, B, Er, Eu, Gd, Tm
2. Linear dose response investigated with TR-OSL method
3. $LiMgPO_4$ doped with 1.2mol% of Tm showed the highest RL by X-ray irradiation

1. INTRODUCTION

Lithium magnesium phosphate ($LiMgPO_4$, called LMP) is a new promising phosphor with a potential to be applied in optically stimulated luminescence (OSL) dosimetry as an alternative to the well-known and routinely used such materials as Al_2O_3:C or BeO. Several groups work on the development of $LiMgPO_4$, usually doped with Tb and B and produced in a form of powder [1-5]. Recently, the investigations have been also performed on crystals grown from LMP powder by micro-pulling down method (MPD) [6-11] or thin foils [12, 13]. In general, LMP is characterized by a high sensitivity to ionizing radiation, good repeatability of the OSL signal, very good linearity of the dose response even from mGy to kGy range [12], but relatively high spontaneous fading in time after exposure. The fading can cause even 20-40% loss of the signal in the first two weeks, with respect to the signal measured immediately after irradiation. Some attempts at reducing the fading, such as pre-heat treatment after irradiation or IR bleaching before readouts have also been undertaken [13]. There were attempts to reduce fading by changing the doping – Menon et al. [12] has obtained for LMP doped only with B the reduction of the fading from 30% to 15%.

While the high fading rate is a serious obstacle for using a luminescent material in typical dosimetric applications, when readout is often performed many weeks after the exposure, there is one field of application in which it is not so crucial problem – the real-time OSL dosimetry. Real-time dosimetry is a measuring technique, which was developed for in vivo dosimetry during radiotherapy [14]. It is based on the use of a point dosimeter in conjunction with an optical fiber, which serves for collecting luminescent signal and for delivering the stimulation light to an OSL detector. The readout is performed immediately after irradiation, therefore fading occurring in a longer time scale has no influence on the results. Detectors dedicated for the application in real-time dosimetry should be characterized by the high sensitivity to the ionizing radiation and small size ensuring good spatial resolutions. The most commonly used detector in this method is Al_2O_3:C [15 - 17] but attempts were also made to apply BeO [18] .

Besides OSL, another effect often used for real-time dosimetry is radioluminescnce (RL), i.e. luminescence emitted during excitation with ionizing radiation. Unlike thermoluminescence (TL) or OSL, which phenomena requires providing some external energy to release trapped charge carriers, RL involves spontaneous recombination of holes and electrons at the luminescence centres. LMP material exhibits strong radioluminescence properties but, with the exception of mention of the construction of real time system for LMP investigation in the article of Gai [19], its characteristic has not been investigated so far.

The general aim of the present work was to study LMP in perspective of its potential application in real-time dosimetry. In order to optimize sensitivity and other properties, the investigations of influence of co-doping with rare earth elements (Tb, B, Er, Eu, Gd) on LMP luminescence were performed. The measurements comprised OSL (both continuous wave and pulsed modes of OSL, as pulsed stimulation is sometimes proposed for real-time dosimetry), RL (under X-ray excitation) and TL (its relationship with OSL).

2. MATERIAL AND METHODS

The subjects of research were the crystals of LMP doped with Tb, B, Er, Eu, Gd, Tm. There were prepared two series of samples. The first one consisted of LMP crystals doped with Tb and B and additionally one of Er, Eu, Gd or Tm. Activators were added in such a way that the total concentration of rare earth elements was always kept constant (0.8 mole percent) and the addition of another dopant resulted in the proportional decrease of Tb concentration (see Table 1, samples #1-5). The second group of crystals was then prepared to study in more detail some aspects of results, mainly the role of Tm dopant (Table 1, samples #6-9).

Table 1. Crystals and concentration of the dopants

Crystal No	Type and content of dopants		
	Tb [mol%]	B [mol%]	additional dopant - mol%
#1	0.8	10	-
#2	0.6		Er – 0.2
#3	0.6		Eu – 0.2
#4	0.2		Gd – 0.6
#5	0.2		Tm – 0.6
#6	0.2		-
#7	0.2	-	Tm-0.6
#8	-	-	-
#9	-	-	Tm- 1.2

The crystals were grown by micro-pulling down method at the facility installed in Institute of Nuclear Physic Polish Academy of Sciences (Krakow). The method and growth condition are described in the work of Kulig et al. [10]. As the starting material the doped LMP in the form of powder was used, which was obtained by a long chemical synthesis procedure described also in the paper of Kulig et al. [10]. The activators were added during the synthesis in the form of following compounds: Er_2O_3, Eu_2O_3, Gd_2O_3 or Tm_2O_3 and H_3BO_3. The obtained crystals had shape of thin (2-3mm in diameter) rods of 5-6 cm length, which were then cut with a diamond wire saw to slices of the thickness of about 1.2mm. The samples (slices of crystals) were opaque white.

The preliminary investigations of TL glow curves and CW-OSL decay curves for all new grown crystals as well as all irradiations were performed in the Risø automated TL/OSL reader DA-20. The reader is equipped with infrared (870 nm) and blue (470 nm) LED stimulation modules and two built-in radiation sources, namely $^{90}Sr/^{90}Y$ and ^{241}Am for irradiation of the samples. Beta particles with the dose rate of about 64.6 mGy/s and maximum beta particles energy of 2.27 MeV were applied for irradiation of samples. Information about the dose rate is based on the calibration performed with the 0.9 mm thick LiF:Mg,Cu,P (MCP) detectors.

The OSL measurements under pulsed mode of stimulation (POSL), as well as radioluminescence measurements, were conducted in one of the portable HELIOS readers series [20], in this case called HELIOS-3, the stimulation and detection paths of which are easily adjusted according to the current needs. For POSL the detectors were excited using 3 blue LEDs (light power 5 W), which emits light of a wavelength of 460 nm. HELIOS-3 is equipped with a Hamamatsu H8259 photon counting gated photomultiplier (PMT) and optical filter UG11 (Schott). The diode current was 20mA. The configuration of HELIOS-3 stimulation and detection paths are intentionally similar to that of Risø TL/OSL reader system configuration. During RL measurements another configuration of the filters was used and this is described in the section 3.3.

The pulsed stimulation enables time resolved registering of the OSL signal (so called "boxcar" mode). The luminescence signal intensity obtained after a single stimulation pulse is very weak and the signal should be accumulated over several pulses to obtain a reasonable signal to noise ratio. The measurements were performed with the following parameters: stimulation time 1 ms, sampling period 0.1ms, number of repetitions 100.

The readouts of POSL in HELIOS-3 were performed always 2 minutes after finishing of the irradiation which were performed in the Risø reader. This time was needed for the transportation of the samples between readers and was always constant in order to avoid any fading effects.

HELIOS-3 reader housing gives the possibility to attach a mini X-ray generator with a Be window, as illustrated in Figure 1. The device was produced in National Centre for Nuclear Research in Warsaw [21]. The dose rate at the sample position under PMT was found to be of (62±10) mGy/min for voltage and U=20kV and current I=20mA). The dose rate was measured by means of LMP detectors irradiated with a calibration dose of 200mGy in the Risø reader. and irradiated with X-ray tube by 5 minutes (this procedure was repeated 3 times). The relatively high deviation of the measured value (SD=16%) can be caused by the inaccuracy of the sample position in relation to the position of the X-ray tube and the handling of the samples between two readers. In spite of this, X-ray tube can be applied for RL measurement in situ in HELIOS-3.

The samples were bleached in the Risø reader between each measurement by the following procedure: firstly the OSL readout with blue diodes for 100s, then twice TL readout up to 500^{o}C with the heating rate of 5^{o}C/s and again OSL readout with blue diodes for 100 s.

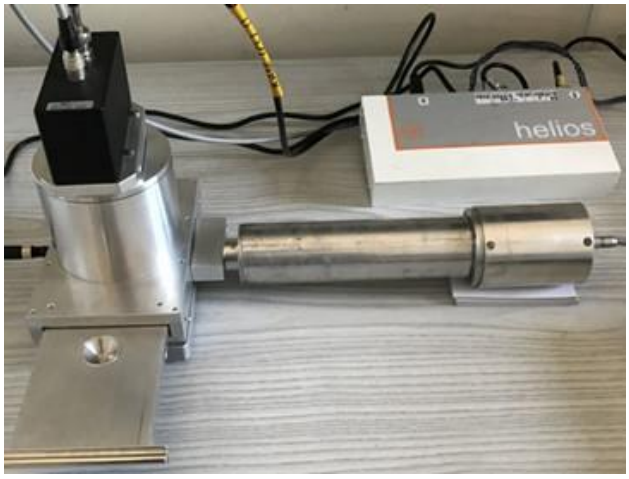

Fig. 1 A photo of HELIOS-3 reader with a mini X-ray generator.

3. RESULTS

3.1 CW-OSL and TL

The OSL decay curves recorded in CW-OSL mode with the Risø reader are presented in Fig. 2. The lowest OSL signal was observed for the crystal doped with Eu (#3), while the highest for the crystal doped with Gd (#4). The insert diagram shows the first 20 seconds of the CW-OSL readout normalized to the first datapoint. As it is seen in this figure, the character of the OSL decay is similar independently of the doping.

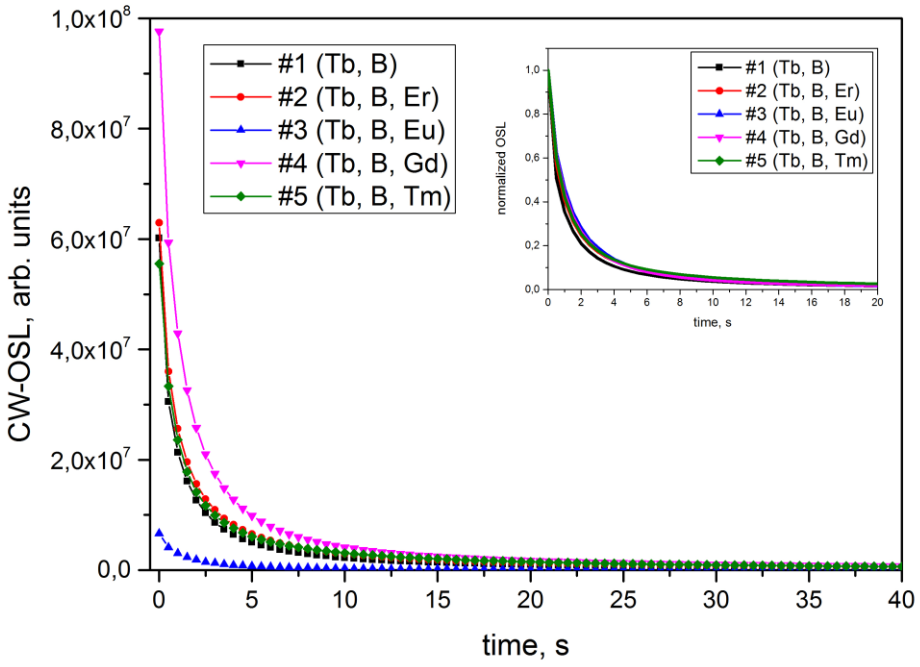

Fig. 2 CW-OSL recorded for crystals #1-5 in Risø reader with the blue diodes stimulation after crystals irradiation with 200 mGy of beta rays. Insert – OSL signals normalized to the first point.

Figure 3 presents TL glow curves of the investigated crystals, recorded at the heating rate of 2°C/s after irradiation with 200mGy of beta particles. All curves have the low temperature peak at about 90°C. According to the work of Menon et al. [12], this peak is connected with the presence of B doping. The amplitude of this peak in the crystal #3 is the lowest (the curve is 10x multiplied in Fig. 3 to expose the shape of the curve). In the case of the crystal doped with Tm (#5) the high temperature peak appearing at 325°C exhibits the highest amplitude among all crystals.

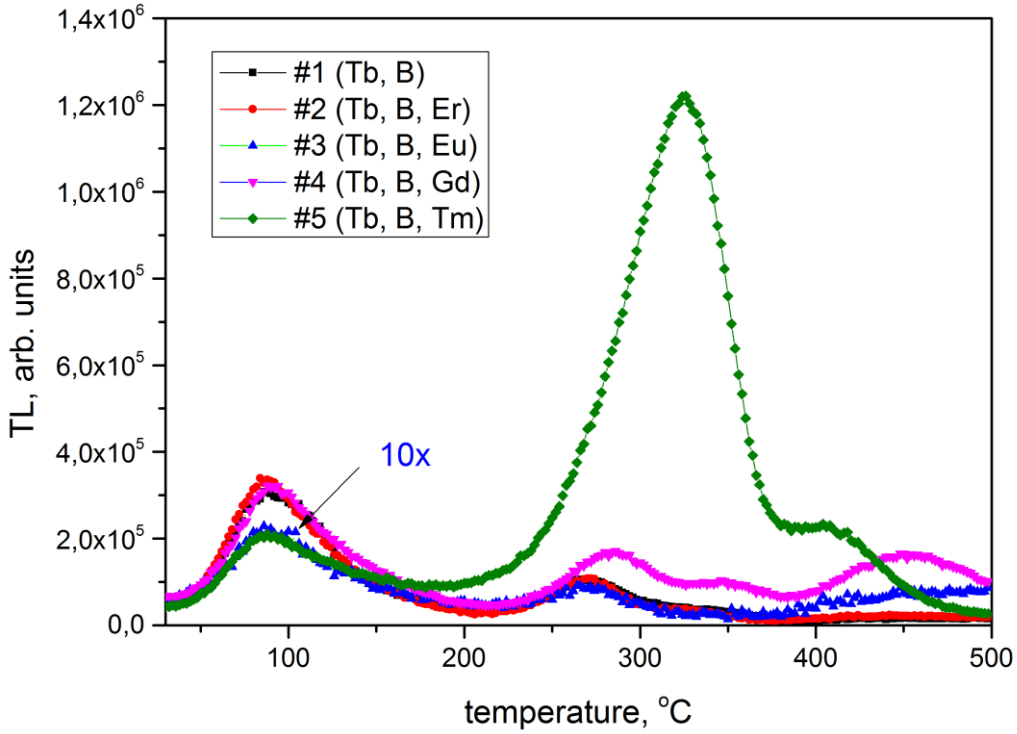

Fig. 3 TL glow curves for all investigated crystals after irradiation with 200mGy of beta particles in Risø reader. Heating rate of 2oC/s. The amplitude of curve for crystal #3 doped with Tb, B, Eu is 10 times multiplied.

In the next step the relationship between traps involved in TL and OSL phenomenon was investigated by successive TL readouts after OSL treatments with different stimulation times: 60 s, 120 s, 300s, 600 s, and conversely, OSL readouts were preceded by preheats up to temperatures ranging from 50 °C up to 500°C, in steps of 50°C. These measurement should explain if the same traps are responsible for TL and OSL phenomena. All TL/OSL measurements were performed in the Risø reader. Before each treatment, all samples were bleached (the procedure was described in MATERIAL AND METHODS) and then irradiated with 200mGy of beta particles.

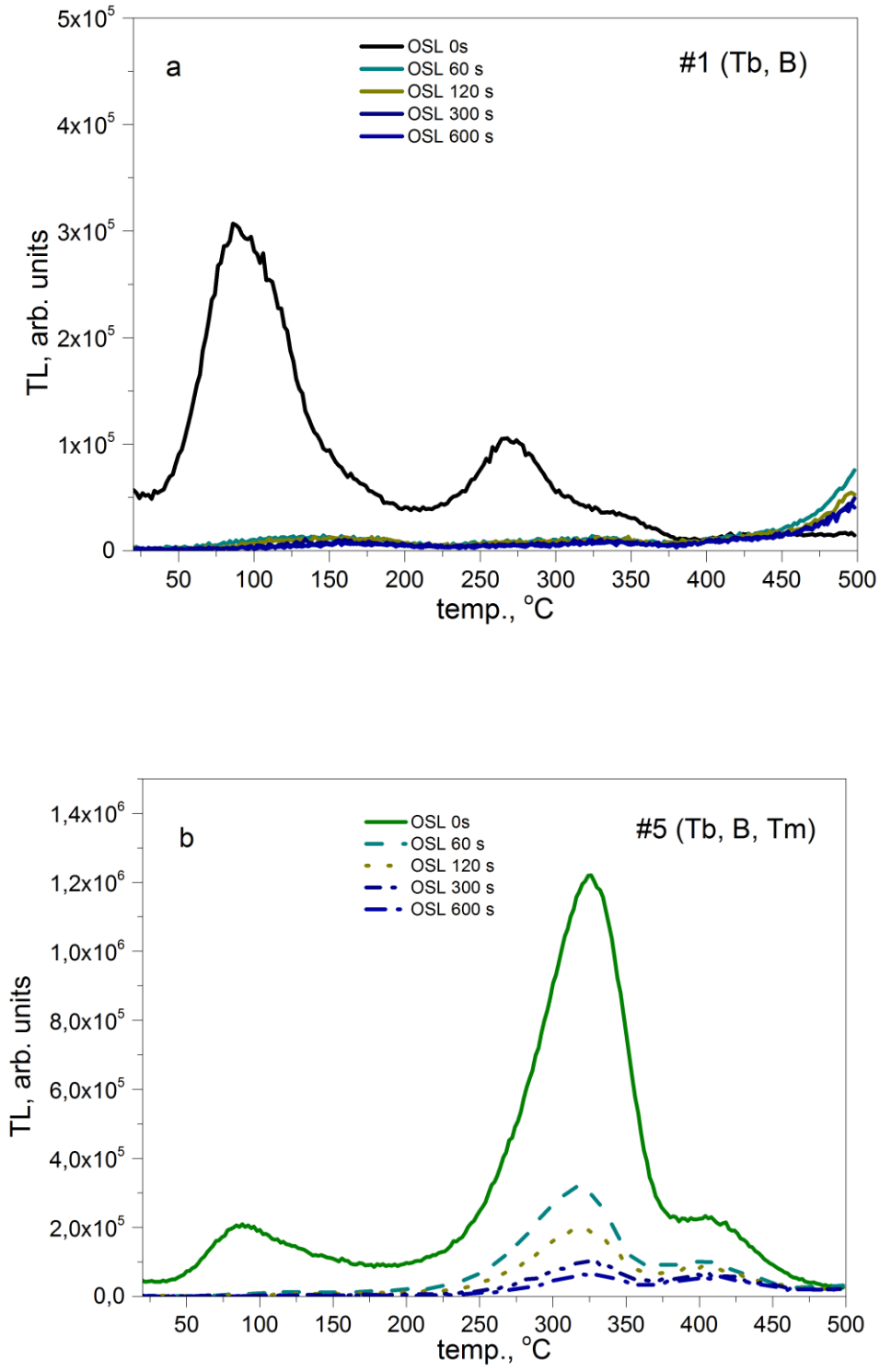

Fig. 4 TL glow curves for crystal #1 doped with Tb, B (a) and #5 doped with Tb, B, Tm (b) after stimulation with blue light. Heating rate of 2°C/s.

The successive stimulations with the blue light in Risø reader (Fig. 4) with the longer periods of time (60 s, 120 s, 300 s and 600 s) caused the decrease of all TL peaks. In the case of crystals #1-4 even 60s of blue light stimulation leads to vanishing of the TL peaks, as it is seen in Fig. 4a. Only crystal #5 doped with Tm showed still the presence of residual high temperature peak at 325 ^{o}C after stimulation with a blue light for 600s (Fig. 4b), but it also decreases with stimulation time, what suggests the same trapping mechanism for both TL and OSL.

Figure 5 presents the example CW-OSL decay curves obtained after heating up to 500^{o}C, in steps of 50 ^{o}C crystals doped with Tb, B (#1) and Tb, B, Tm (#5). It is apparent that even a small rise of the temperature causes a decrease of OSL decay curves. Pre-heat to 350 ^{o}C reduces the signal to the background level (it should be also noted that the Tm doped samples show several times higher background that other crystals). In order this effect, the OSL signal was integrated over the whole measuring period (600 s) and presented as the function of the preheat temperature (Figure 6). This plot shows that the OSL signal decreases with increasing temperature up to 300-350°C. This temperature range corresponds to positions of all TL peaks (with exception of the peak at about 420°C for crystal #5). It should be also mentioned the level reached by the OSL signal for preheat temperatures >300°C is much higher than the background signal od unirradiated crystals. It seems therefore that this signal is related to some deep traps which are not emptied even at 500°C. The highest level of the CW-OSL sums for pre-heat temperatures above 350^{o}C results from the general higher background signals for samples doped with Tm.

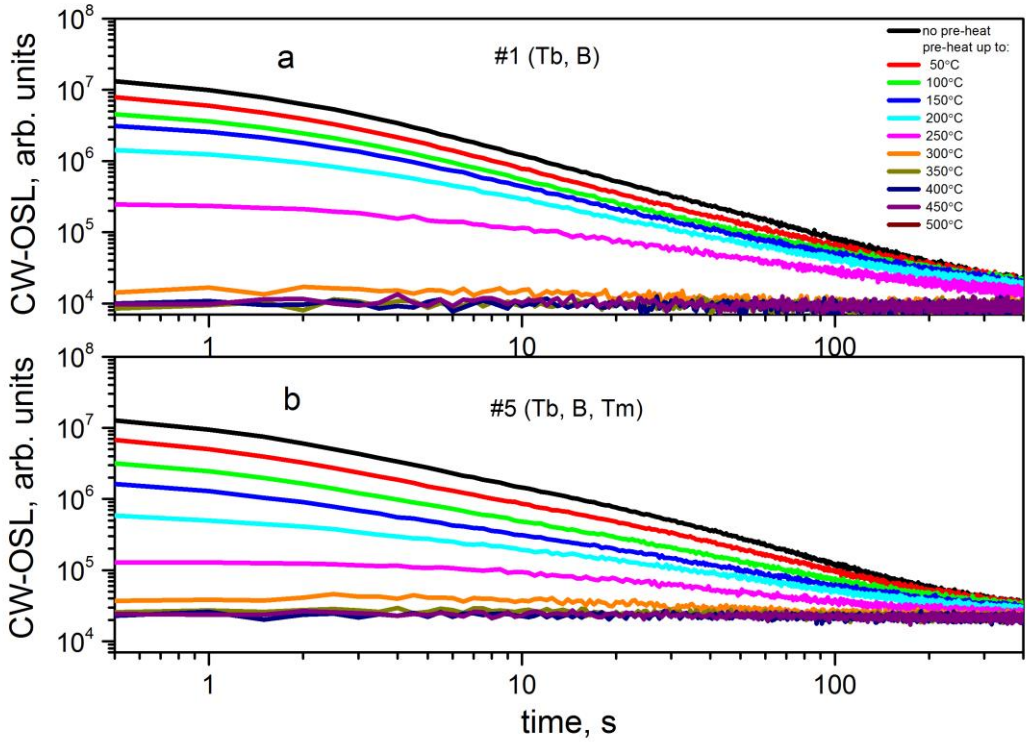

Fig. 5 CW-OSL decay curves after heating up to successive pre-heat temperatures, a- for crystal #1 doped with Tb, B; and b- for crystal #5 doped with Tb, B, Tm.

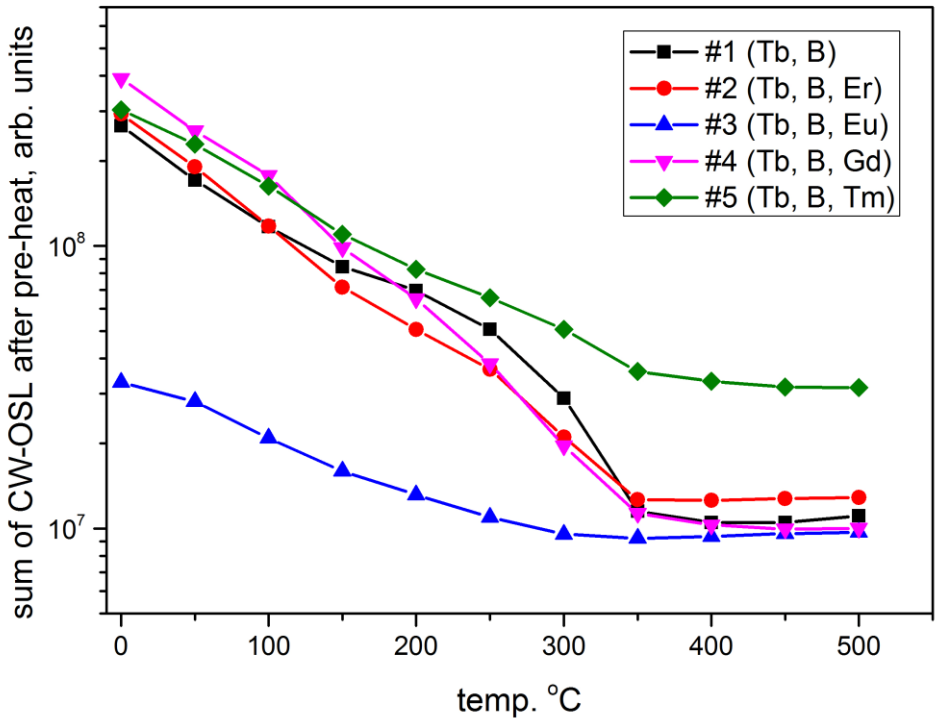

Fig. 6 Sum of CW-OSL signal as the function of nominal pre-heating temperatures for crystals #1-5.

3.2 TR-OSL

TR-OSL measurements were performed in HELIOS-3 reader for the crystals #1-5 irradiated in Risø reader. Figure 7 presents the representative curves obtained for all investigated samples after irradiation with 10 Gy of beta particles. In comparison with the Fig. 2 the difference between CW and POSL modes of OSL readouts is visible. The highest CW-OSL signal was detected for crystal #1 doped with Tb, B and the lowest for crystal #3 doped with Tb, B, Eu. In the POSL mode also the crystal #3 doped with Eu had the lowest signal and the crystal #1 doped only with Tb, B showed the highest signal. The emission of the light during stimulation (CW-OSL) and after stimulation (POSL) depends on the kind of crystal.

In the next step the crystals were irradiated with the doses from 0.5 Gy up to 10Gy of beta particles to investigate their dose response. The irradiations were performed in Risø reader with $^{90}Sr/^{90}Y$ source and the samples were transported to HELIOS-3. Before each irradiation the samples were bleached according to the described procedure.

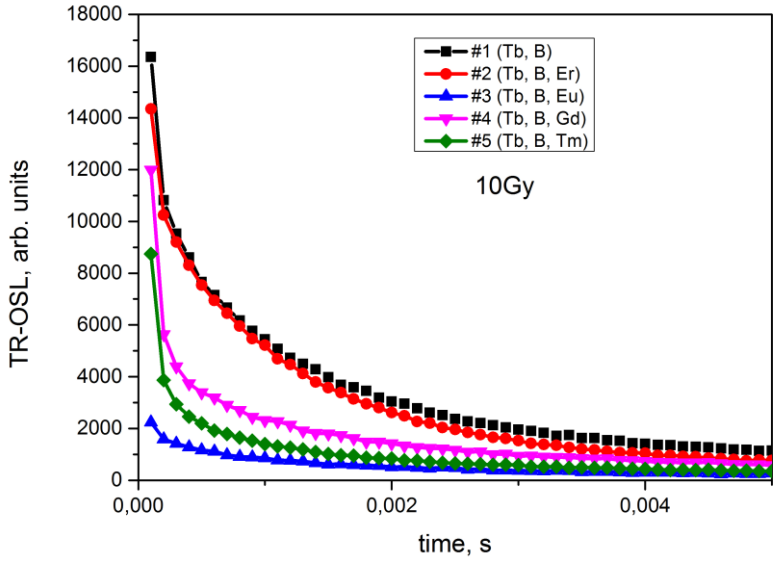

Fig. 7 TR-OSL of LMP samples stimulated with the pulse of 10^{-3}s and sampling period of 10^{-4} s recorded in HELIOS-3 reader. The samples were irradiated with 10Gy of beta particles.

To compare the character of the decay curves, next figure (Fig.8) presents the normalized TR-OSL for the doses of 0.5Gy and 10Gy (insert) for the first group of the investigated crystals. It is seen that the curves are divided into two groups: LMP doped with Gd and Tm with the faster decay of the curves (amplitude decrease by half in 0.2 s) and the rest of the curves with the slower decay (amplitude decrease by half in 0.4 ms) in the first sampling periods .

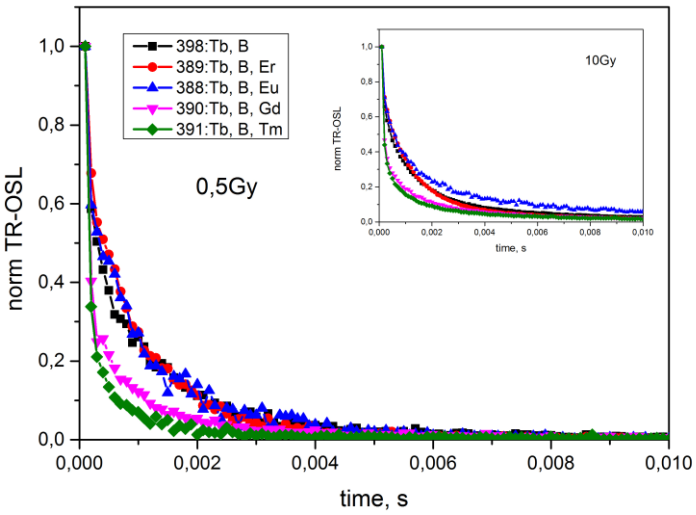

Fig. 8 Normalized TR-OSL signal for LMP crystals irradiated with dose of 0.5 Gy and 10 Gy (insert) of beta particles.

The dose response of the LMP crystals in the dose range 0.5-10 Gy is presented in Figure 9. The obtained curves confirm the linear character of the dose response in this range of doses for all crystals (R^2=0.99) except crystal #4 doped with Tb, B, Gd for which R^2 was 0.93.

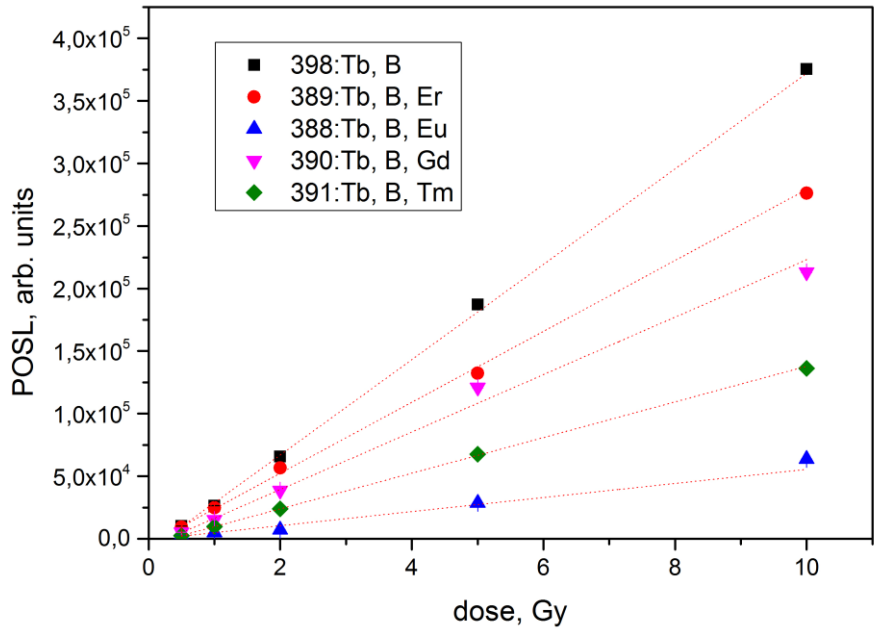

Fig. 9 Dose response measured by TR-OSL in HELIOS-3 reader for crystals irradiated with beta particles in Risø reader.

TR-OSL – repeatability of the signal

To check the repeatability of the TR-OSL signal several cycles of irradiation and bleaching procedure were performed. Figure 10 presents the results of 8 readouts of sample doped with Tb, B (crystal #1) irradiated with 10Gy of beta rays. The SD of TR-OSL discrepancy was 5.3%. The reason of such discrepancy can be the fact that the irradiations were done outside at the beta source in Risø reader, despite transportation of the samples between the Risø reader and HELIOS-3 in darkness and keeping the 2-minute time regime.

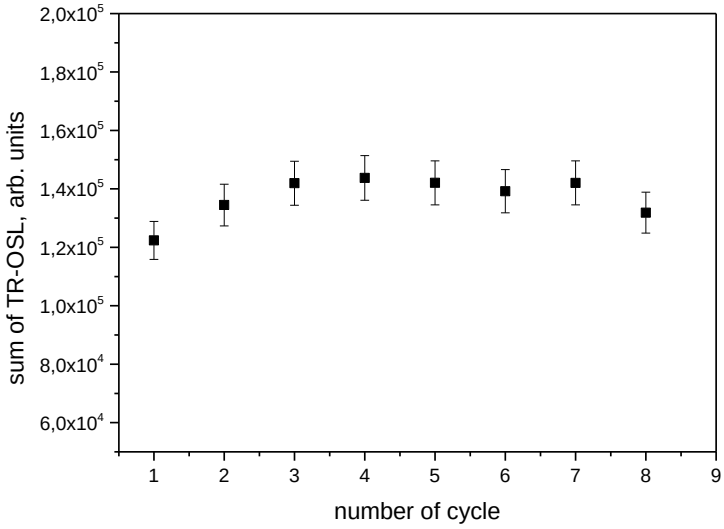

Fig. 10 Repeatability of the POSL measurement for crystal #1 doped with Tb, B irradiated with 10Gy of beta particles. Before each irradiation cycle a bleaching procedure was performed (firstly the OSL readout with blue diodes for 100s, then twice TL readout up to 500^{o}C with the heating rate of 5^{o}C/s and again OSL readout with blue diodes for 100 s).

3.3 RL measurements

As it was observed in the preliminary measurements, LMP crystals emit spontaneously the radioluminescence during irradiation. To check this phenomenon, the housing of the HELIOS-3 reader was adapted for installing of the mini X-ray tube to enable the measurement of RL during irradiation (Figure 1). Fig. 11 present the results of the X-ray irradiation with the dose rate of (62±10) mGy/min at the sample position. After 5 minute irradiation the X-ray tube was switched off and stimulation was started to record CW-OSL for next 5 minutes. It can be assumed that 5 minute irradiation with X-ray tube gives the dose of about 310 mGy. It should be also noted that the RL was recorded for the emission detected in the wavelength range 240 nm-400 nm. In this condition the signal of crystal #5 doped with Tb, B, Tm sample is the highest in contrast to CW-OSL signal which is lower than that of #3 doped with Tb, B, Er. In the cases of RL and CW-OSL the signal of crystal #3 is the lowest. The RL signals were normalized to the mass of the samples. All investigated samples (except of crystal #3) showed relatively high RL and CW-OSL signal emitted in the 240-400 nm wavelength which may be not optimal for this kind of the luminophore.

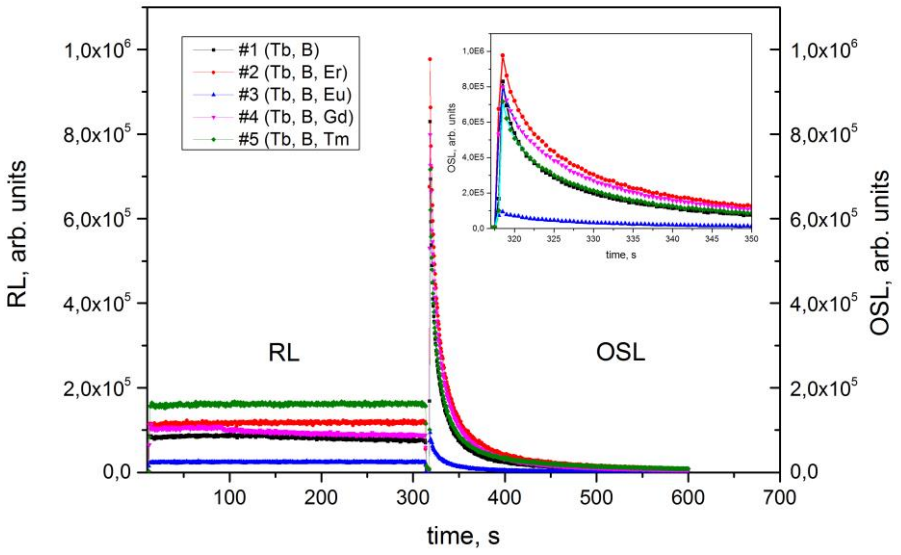

Fig. 11 RL signal emitted during 5 minute irradiation with mini X-ray generator and CW-OSL recorded immediately after finishing of irradiation (of about 310 mGy) for LMP crystals. Emission recorded for the spectral range 240-400 nm.

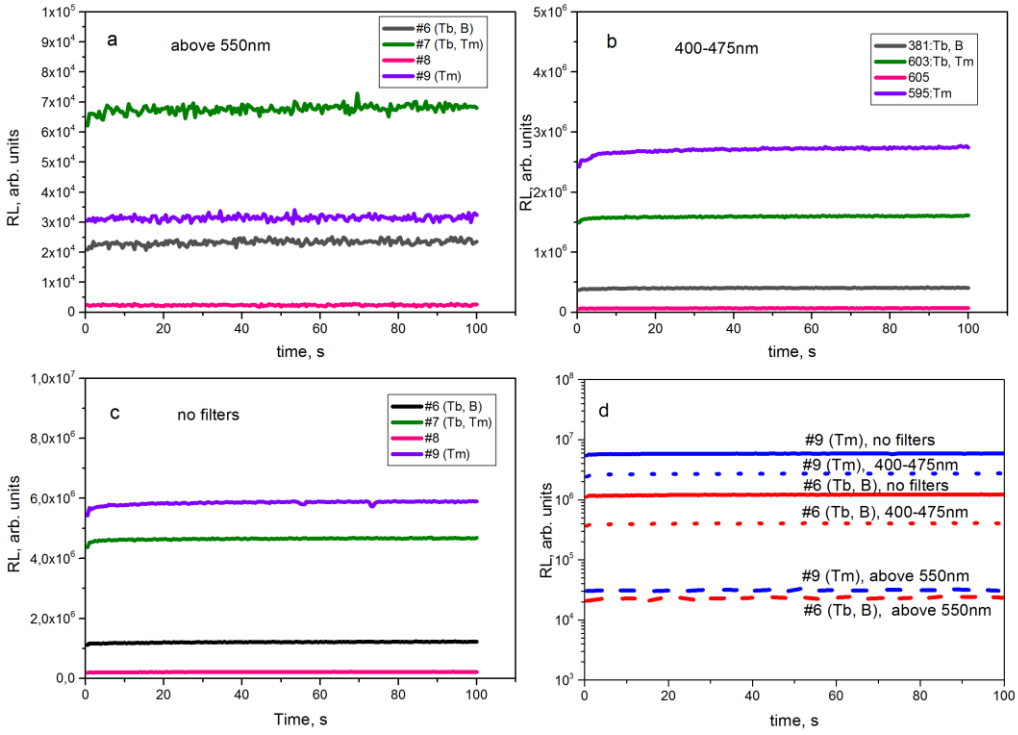

Fig. 12 RL signal emitted during 100s irradiation with mini X-ray generator, emission recorded for the emission above 550 nm (a), 400-475 nm (b), full range (no filters, c) and comparison of RL for crystals #6 doped with Tb, B and I#9 doped with Tm, in different filter configurations (d).

The highest RL signal found for the samples doped with Tb, B, Tm (crystal #5) encouraged to perform more detailed investigations on the influence of Tm and Tb dopants, by changing doping. Therefore the next part of RL investigations focused on the second group of the crystals, namely: #6 doped with 0.2Tb, 10B; #7 doped with 0.2Tb, 0.6Tm; #9 doped with 1.2Tm and undoped crystal #8.

RL measurements described above referred to the filter configuration applied in Risoe reader, i. e. the measurement was carried out in the range of 240 nm-400 nm. In next part of experiment, RL measurements were conducted in another wavelength ranges, planned for the future use of green light stimulation instead of the blue one. The irradiation with the mini X-ray tube lasted 100 seconds and RL measurements were carried out with three different filter configurations: transmitting light with the wavelength longer than 550 nm (Figure 12a), transmitting light between 400-475 nm (Fig. 12b) and without any filter (Fig. 12c). For the detection of the light emission above 600nm some limitation can be imposed by the spectral characteristic of the PMT applied in HELIOS-3 for which the count sensitivity starts to decrease above 400nm and the fall is getting more steeper above 600 nm. The RL signals were normalized to the mass of the samples. Initial signal increase in the first 5-8 seconds can be caused by the warming of the X-ray generator before its stabilization because the X-ray tube and the recording of the PMT were started at the same time.

As it is seen in the Figure 12, the highest signals was obtained for the samples containing Tm dopant in all cases of the filtration. The RL signal of crystal #9 is 24 times higher as RL signal of undoped sample, by the level of the background at 400 impulses for the configuration with no filter (160 and 5 for 400-475 nm filter and above 550 nm, respectively). The lowest RL signals for all investigated crystals were recorded for the emission above 550 nm but in this case the relatively higher signal was noticed for crystals doped with Tb. This is in agreement with the spectra position of the emission peaks for crystals doped with Tb (418 nm, 440 nm, 460 nm, 486 nm and the shoulder of 552 nm peak) and Tm (460nm) [19, 22].

Taking in consideration only the crystals #6 doped with Tb, B and #9 doped with Tm (Fig. 12d) we can tell that for the sample doped with 1.2 mol% of Tm it can be obtained 5 time higher RL signal than for the sample doped with Tb and B, independently from the applied filtration, what means that the Tm doping is very effective for RL signal.

The measurements carried out with X-rays showed the high potential of the LMP crystals in regard to their application in real time dosimetry due to their very small size (1-3mm^3) and very high RL signal as well as high OSL signal, both in CW and TR modes. The applied X-ray generator didn't give the possibility to use different dose rates due to its instability at higher voltage and current, but the investigation will be continued with another radiation sources.

CONCLUSSIONS

Investigated LMP crystals doped with rare earths elements such as Tb, B and Er, Eu, Gd or Tm can be successfully used as OSL detectors both in CW and TR mode, where the sensitivity in these modes of operation is different for the particular crystals. In TR-OSL mode the most sensitive samples were the crystals #1 doped with Tb, B and #2 doped with Tb, B, Er, in CW-mode the highest signal was recorded for crystal #4 doped with Tb, B, Gd. All crystals showed the linear dose response in the range from 0.5 Gy till up to 10 Gy. Among all investigated

samples RL signal was the highest for the samples doped with 1.2mol% of Tm for the full emission range (no filter) and for emission in wavelength range of 400-475 nm. Relatively high RL signal recorded for wavelengths longer than 550 nm was measured for crystals doped with Tb what is consistent with spectral emission range of the investigated samples. Tm or Tb doped crystals are the promising candidates for detectors in fiber real time dosimetry due to their very high sensitivity to the ionizing radiation, high OSL and RL signals even for very small pieces (1-3mm^3) of the crystals what can ensure the good spatial resolutions. Further experiments with the changing the doping of LMP crystals as well as the investigation of RL emission by irradiation with different radiation sources at various dose rates are planned.

Acknowledgements: This work was supported by the National Science Centre, Poland (Contract No. UMO-2016/21/B/ST8/00427).

REFERENCES:

[1] S. Zhang, Y. Huang, L. Shi, H. J. Seo, The luminescence characterization and structure of Eu^{2+} doped $LiMgPO_4$, J. Phys.: Condens. Matter 22 (2010) 235402;

[2] M. Kumar, B. Dhabekar, S.N. Menon, M.P. Chougaonkar, Y.S. Mayya $LiMgPO_4$:Tb,B OSL phosphor – CW and LM OSL studies, NIM B 269 (2011) 1849–1854;

[3] B. Dhabekar, S.N. Menon, E. Alagu Raja, A.K. Bakshi, A.K. Singh, M.P. Chougaonkar, Y.S. Mayya, $LiMgPO_4$:Tb,B – A new sensitive OSL phosphor for dosimetry, 269 (2011) 1844–1848;

[4] S.N. Menon, B. Dhabekar, E. Alagu Raja, M.P. Chougaonkar, Preparation and TSL studies in Tb activated $LiMgPO_4$ phosphor, Rad. Meas. 47 (2012) 236-240;

[5] N.S. Bajaj, C.B. Palan, K.A. Koparkar, M.S. Kulkarni, S.K. Omanwar, Preliminary results on effect of boron co-doping on CW-OSL and TL properties of $LiMgPO_4$: Tb,B; J. of Lum. 175 (2016) 9–15;

[6] G. Denis, M. S. Akselrod, and E. G. Yukihara, Influence of shallow traps on time-resolved optically stimulated luminescence measurements of Al_2O_3:C,Mg; Journal of Applied Physics 109, 104906 (2011);

[7] D. Wróbel, P. Bilski, B. Marczewska, M. Kłosowski, TL and OSL properties of $LiMgPO_4$:Tb,B, Oxide Materials for Electronic Engineering (OMEE 2014), DOI: 10.1109/OMEE.2014.6912439;

[8] D. Kulig (Wróbel), W. Gieszczyk, P. Bilski, B. Marczewska, M. Kłosowski, Thermoluminescence and optically stimulated luminescence studies on $LiMgPO_4$ crystallized by micro pulling down technique, Rad. Meas. 85 (2016) 88-92;

[9] D. Kulig (Wróbel), W. Gieszczyk, P. Bilski, B. Marczewska, M. Kłosowski, New OSL detectors based on $LiMgPO_4$ crystals grown by micro pulling down method. Dosimetric properties vs. growth parameters, Rad. Meas. 90 (2016) 303-307;

[10] D. Kulig, W. Gieszczyk, B. Marczewska, P. Bilski, M. Kłosowski, A.L.M.C. Malthez, Comparative studies on OSL properties of $LiMgPO_4$:Tb,B powders and crystals, Radiat. Meas. 106 (2017) 94-99;

[11] B. Marczewska, P. Bilski, D. Wróbel, M. Kłosowski, Investigations of OSL properties of $LiMgPO_4$: Tb,B based dosimeters, Rad. Meas. 90 (2016) 265-268;

[12] S. N. Menon, B. S. Dhabekar, S. Kadam, D. K. Koula Fading studies in LiMgPO4:Tb,B and synthesis of new $LiMgPO_4$ based phosphor with better fading characteristics NIM B 436 (2018) 45-50;

[13] A.L.M.C.Malthez, B.Marczewska, D.Kulig, P.Bilski, M.Kłosowski, Optical and thermal pre-readout treatments to reduce the influence of fading on LiMgPO4 OSL measurements, Applied Radiation and Isotopes 136 (2018) 118-120;

[14] L.F. Nascimento, F. Vanhavere , E. Boogers , J. Vandecasteele, Y. De Deene, Medical dosimetry using a RL/OSL prototype, Radiat. Meas. 71 (2014) 359-363;

[15] E. G. Yukihara, B. A. Doull, M. Ahmed, S. Brons, Th. Tessonnier, O. Jäkel and S. Greilich, Time-resolved optically stimulated luminescence of Al_2O_3:C for ion beam therapy dosimetry; Physics in Medicine & Biology 60, No 17(2015) 6613;

[16] C. E. Andersen, J. M. Edmund, S. M. S. Damkjær Precision of RL/OSL medical dosimetry with fiber-coupled Al_2O_3:C: Influence of readout delay and temperature variations, Radiat. Meas. 45 (2010) 653-657;

[17] S. Buranurak, C.E. Andersen, Fiber-coupled Al2O3:C radioluminescence dosimetry for total body irradiations, Radiat. Meas. 93 (2016) 46-54;

[18] E. Bulur, More on the TR-OSL signal from BeO ceramics, Rad. Meas. 66 (2014) 12;

[19] M. Gai, Z. Chen, Y. Fan, J. Wang, Synthesis and luminescence in LiMgPO4:Tb,Sm,B phosphors with possible applications in real-time dosimetry, J. of Rare Earths 31 (2013) 551-554;

[20] A. Piaskowska, B. Marczewska, P. Bilski, A. Mandowski, E. Mandowska, Photoluminescence measurements of LiF TL detectors, Radiat. Meas. 56 (2013) 209-212;

[21] M. Budzanowski, P. Olko, B. Marczewska, L. Czopyk, M. Słapa, W. Stras, M. Traczyk, and M. Talejko Dose distribution around a needle-like anode X-ray tube: dye-film vs. planar thermoluminescent detectors, Radiat. Prot. Dosim., Vol. 120 (2006) 117;

[22] J.C.G. Bünzli, S.V. Eliseeva, Basics of Lanthanide Photophysics, Lanthanide Luminescence, Springer Series on Fluorescence (Methods and Applications) 7 (2010) 1-45. Springer, Berlin, Heidelberg.